Vol. 41, No. 2 (2019) 220-236, DOI: 10.24874/ti.2019.41.02.08

Tribology in Industry

www.tribology.rs

RESEARCH

Experimental Study on an Influence of Bearing Geometry and TiO_2 Nanoparticle Additives on the Performance Characteristics of Fluid Film Lubricated Journal Bearing

S.R. Suryawanshi[a], J.T. Pattiwar[b]

[a]*Mechanical Engineering Department, MET's IOE, BKC, Nasik, SPPU, Pune, India,*
[b]*SMES SCOE, Nashik, SPPU, Pune, India.*

Keywords:

Experimental test rig
Pressure distribution
Temperature rise
Tribology
Journal bearing

Corresponding author:

Shubham R. Suryawanshi
Mechanical Engineering Department, MET's IOE, BKC, Nasik, SPPU, Pune, India.
E-mail:
shubhamsuryawanshi255@gmail.com

A B S T R A C T

The objective of this article is to study the performance characteristics of the journal bearing experimentally having different geometries operating with commercial Mobil grade lubricants that are used in power plant. Three grades of Mobil lubricants (DTE 24, DTE 25, and DTE 26) have been considered during the study. TiO_2 nanoparticle additives have also been considered during the study as a lubricant additive to examine the performance of journal bearings. An analytical approach was presented in the author's earlier work to obtain pressure and temperature profile. The dynamic characteristics such as stiffness and damping properties of journal bearings are represented in this paper. An experimental test rig is developed to accommodate any geometrical type of bearing. An elliptical journal bearing shows the superior performance than that of a plain bearing. The obtained experimental results are in a very good agreement with theoretical results for pressure and temperature profile.

1. INTRODUCTION

The rotating types of machinery are operating with an integral part known as hydrodynamic journal bearing of fluid film journal bearing. These journal bearings consist of stationery cylindrical bearing in which the journal rotates at a certain speed. The lubricating oil is supplied in the clearance space between the journal and bearing surface. The whirl instability phenomenon occurs during the operation of the journal bearing system that changes the properties of lubricating oil. This is due to the heat generation in the system that eventually causes the temperature rise in the oil film of lubricating oil. This phenomenon tends to cause the metal to metal contact during running condition. Hence the action of whirl instability may lead to the damage of the system. It decreases the performance of the bearing and affects the lubricant viscosity as it depends on the temperature [9]. Many researchers are

carrying out research on the stability analysis of the journal bearing system, as it is the crucial area of the dynamics. However, the concept of instability created by oil whirl is not very clear. This needs a better understanding of the oil whirl and whip phenomenon to identify the fault in the system. To overcome the difficulties during the operation of the journal bearing system, this study promotes the performance evaluation of non-circular fluid film lubricated journal bearings operating with nanoparticle-based lubricants. An elliptical journal bearing has been considered as a non-circular shaped journal bearing to investigate the performance of journal bearing over the plain circular journal bearing. This paper extends the author's analytical work [9,23] using the experimental methodology. The experimental analysis has been presented in this work to investigate the performance of the journal bearing with a wide range of operating conditions. The dynamic performance characteristics such as stiffness and damping coefficients are computed analytically in this work. Some of the following researchers have provided a study on the performance characteristics of the journal bearing system. Brito et al. [1] carried out the comparative analysis by an experimental method for the journal bearing system with one and two grooves respectively. The flow rate and temperature rise were reduced effectively with an increase in load and angle respectively as the number of grooves increased. Dhande and Pande [2] have presented a study based on an experimental approach considering a cavitation phenomenon. An effect of speed on the cavitation was presented in the range between 1000 to 5000 r.p.m. Cristea et al. [3,8] have experimentally performed the analysis on journal bearing from steady state to thermal stable state. The temperature and pressure profiles were plotted across the bearing surface at a wide range of oil flow rate and frictional torque. Mishra et al. [4] have studied the different contour plots for temperature in an elliptical (lobed) bearing. From the results, it was summarized that due to an elliptical geometry of the bearing, the temperature gets reduced and the cooling effect was also produced, but at the same time, the pressure distribution got hampered to some extent. Sehgal [5] investigated an offset half & elliptical journal bearing considering the thermal effects. The performance analysis was carried out on various grades of oils and speeds to identify the effect on temperature profile, pressure & Sommerfeld number. Binu et al. [6,10] performed a study to determine the performance parameters for circular journal bearing operating with nanofluid having TiO_2 as a nanoparticle additive in the lubricating oil. Experimental analysis was carried out using SAE 30 as a lubricant. Kasai et al. [7] analyzed the performance of the bearing operating with polymer contained oils. Babbitt and bronze materials were considered as bearing material. The performance of the bearing system was improved due to the influence of the polymer. As compared to the base oil, the pressure distribution was increased and friction was reduced when the bearing was operated with polymer contained oils. Suryawanshi and Pattiwar [9] presented the performance analysis for a plain and an elliptical journal bearing operating with industrial lubricants. Titanium dioxide nanoparticle of size 40 nm was used as a lubricant additive to examine the performance of the bearing. Comparative analysis was carried out for three different lubricants with titanium dioxide (0.5 %wt) nanoparticles. Influence of titanium dioxide as an additive on the performance characteristics of the journal bearing such as pressure distribution, load carrying capacity, attitude angle, power loss, oil flow rate, side leakage, frictional force and temperature rise in a film was examined. Further, the researchers have investigated the physicochemical properties of the lubricants [23]. In this paper, the tribological properties of selected lubricants were studied in detail and enhanced significantly with TiO_2 nanoparticle additives in the lubricant. The physical, chemical and thermal properties of lubricants were improved after the addition of TiO_2 nanoparticle additives in the lubricant. The tribochemical reaction film was formed between ball surfaces during the experiments on four ball tester that minimizes the asperity contact. Baskar et al. [11] described the influence of CuO, TiO_2 & WS_2 nanoparticles on the performance of chemically modified rapeseed oil (CMRO). The anti-wear and frictional characteristics were analyzed using a four-ball tester machine. Amongst selected nanoparticles, CuO nanoparticles as an additive showed better performance as the coefficient of friction and wear scar diameter were reduced significantly for CMRO lubricant. Li et al. [12] studied the tribological behaviour of

CeO_2 and ZrO_2 nanoparticle additives on the performance of the ta-C coating. CeO_2 nanoparticle additives have resulted in better anti-wear and ZrO_2 nanoparticle additives have resulted in better anti-friction properties during the study. Bongfa et al. [13] investigated the tribological performance of crude Nigeria-based castor oil using the four ball tester to propose it as better lubricating oil than the mineral oil-based crankcase oils in the market. Gunnuang et al. [14] analyzed the performance of journal bearing using Al_2O_3 nanoparticles. Carreau viscosity model was implemented in the study for multigrade engine oil SAE 10W50. Results revealed that the load carrying capacity was increased after addition of Al_2O_3 nanoparticles but the film temperature remained almost the same. Solghar [15] have also taken Al_2O_3 as a lubricant additive in the base oil. The coefficient of friction and load carrying capacity were increased whereas the flow rate was decreased after addition of Al_2O_3 nanoparticles. Shenoy et al. [16] considered API-SF engine oil blended with three different nanoparticles such as nano-diamond, titanium dioxide (TiO_2) and copper oxide (CuO) to analyze the performance of the fluid film journal bearing. Out of three nanoparticle additives, TiO_2 showed the best performance for static characteristics. The load carrying capacity and friction were increased while end leakage was decreased significantly for journal bearing. Nicoletti [17] investigated the thermal properties and static characteristics of hydrodynamic journal bearing operating with nanolubricants. Six various nanoparticles Si, SiO_2, Al, Al_2O_3, Cu and CuO were taken in the study with ISO VG 68 as a base fluid. It was observed that the volumetric heat capacity was increased with the addition of nanoparticles in the base fluid. Amongst six nanoparticles, the lubricant that contains CuO nanoparticles was found better to achieve higher volumetric heat capacity. Montazeri [18] focused on his research work based on ferrofluid as a lubricant using numerical and CFD technique. An effect of magnetic field on the performance of a bearing system was investigated. It was found that the attitude angle and load carrying capacity were increased effectively whereas the coefficient of friction was decreased when the bearing was operating with ferrofluid as a lubricant. Kushare and Sharma [19,20] exhaustively studied the hybrid journal bearing which had two lobes operating with non-Newtonian lubricants. It was convinced that the offset factor in multi-lobe bearings influences the performance parameter as well as the stability of a system. The study based on surface roughness was conducted with respect to parameters for a range of offset factors. Wang et al. [21] considered a couple stress fluid as a lubricant to carry out thermohydrodynamic analysis. When journal bearing was operated with a couple stress lubricant, the load carrying capacity and frictional force were increased whereas the coefficient of friction was reduced. It was observed that the side leakage flow remained constant with couple stress lubricant. Aimen and Syahrullail [22] proposed a palm oil blended oil for engine oil over the mineral oil-based lubricant. Tribological properties were improved with the palm oil blended oil that tested with the help of four-ball tester.

A thorough study of the literature reveals that few researchers have focused on performance analysis of journal bearing operating with nanolubricant using an experimental method. Thus, this research work is aimed to bridge the gap in the literature by developing the journal bearing test rig for performance analysis. A plain circular and an elliptical bearing are considered in this study to identify the influence of bearing geometry on the performance. Titanium dioxide (TiO_2) nanoparticles of size 40 nm and having 0.5% wt. have been considered as additives in three grades of lubricating oils. Theoretical analysis is presented in the author's previous work in detail. The static characteristics such as pressure and temperature rise in the oil film are validated using an experimental test rig that is specially designed to accommodate any type of bearing configuration. In addition to this, dynamic performance characteristics such as stiffness and damping coefficients are also computed and discussed in this paper. The results obtained in this paper are expected to be helpful to the bearing designers, researchers and academicians concerned with the relevant study.

2. MATERIAL AND METHOD

The schematic view for a plain bearing is presented as shown in Fig. 1. Reynolds's equation in two-dimensional form for hydrodynamic journal bearing is expressed as [2]:

$$\frac{U}{2}\frac{\partial h}{\partial x}-\frac{1}{12\mu}\frac{\partial}{\partial x}\left(h^3\frac{\partial p}{\partial x}\right)-\frac{1}{12\mu}\frac{\partial}{\partial z}\left(h^3\frac{\partial p}{\partial z}\right)=0 \quad (1)$$

Extending the above equation leads to the following expression:

$$\frac{\partial}{\partial\theta}\left(\frac{h^3}{12\mu}\frac{\partial p}{\partial\theta}\right)+R^2\frac{\partial}{\partial z}\left(\frac{h^3}{12\mu}\frac{\partial p}{\partial z}\right)=\frac{UR}{2}\frac{\partial h}{\partial\theta}+\frac{V}{R^2}+\frac{h}{2R^2}\frac{\partial U}{\partial\theta}\frac{\partial h}{\partial t} \quad (2)$$

For design purpose, it is sufficient to estimate the temperature rise of the fluid ΔT. This estimation is based on the simplified assumption that it is possible to neglect the heat conduction through the bearing material in comparison to the heat removed from the continuous replacement of fluid.

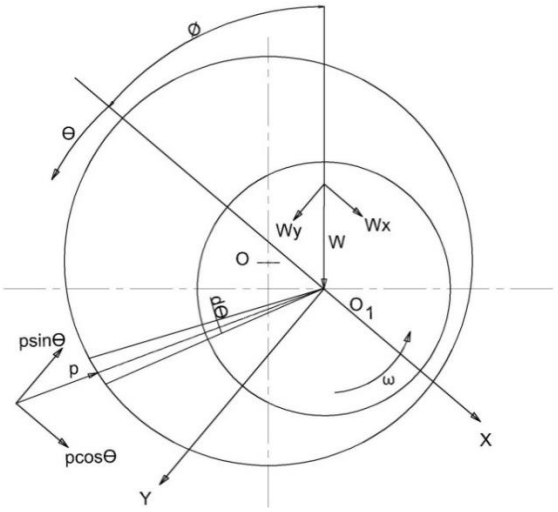

Fig. 1. Components of hydrodynamic force.

The following equation is used to compute the temperature rise in a fluid film [24]:

$$\Delta T=\frac{8.3P\left(\frac{fR}{C}\right)}{10^6\left(\frac{Q}{nRCL}\right)\left(1-0.5\frac{Q_S}{Q}\right)} \quad (3)$$

The dimensionless parameters like $\frac{Q}{nRCL}$, $\frac{Q_S}{Q}$ and $\frac{fR}{C}$ are referred from the Raimondi Boyd chart. The values of these dimensionless parameters for the various intermediate eccentricity ratios are computed using a linear interpolation technique.

2.1 Equations for an elliptical bearing

The elliptical journal bearing consisting of two lobes is represented in Fig. 2. The attitude angles for upper lobe and lower lobe are denoted by ϕ_1 and ϕ_2 respectively.

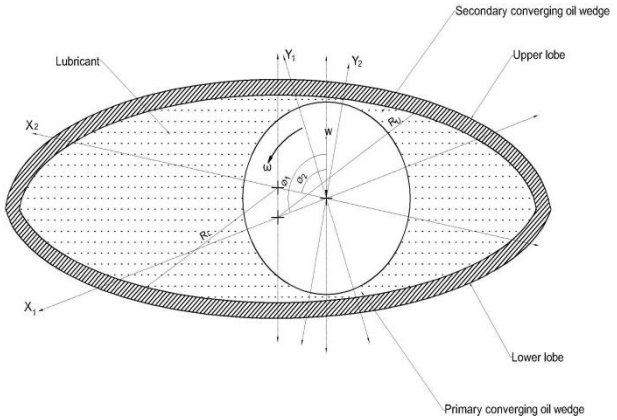

Fig. 2. Geometry of an elliptical journal bearing.

Table 1. Geometrical and operating parameters for bearing.

Parameter	Value
Journal diameter, D	50 mm
Bearing length, L	50 mm
L/D ratio	1
Clearance, C	0.05 mm
Type of lubricant	Mobil grade (DTE 24, DTE 25,DTE 26)
Journal speed, N	500 -1000 r.p.m.
Load, W	1000 N
Clearance ratio, C/R	0.002
Preload ratio for an elliptical bearing, m	0.5
Major diameter of an elliptical bearing	50.3 mm
Minor diameter of an elliptical bearing	50.2 mm
Elliptical ratio, E_m	0.5

The oil film thickness is computed as [5],

$$h=C_m[1+E_m+\varepsilon_1\cos(\theta+\phi-\phi_1)] \text{ for } 0°\le\theta\le180° \quad (4)$$

$$h=C_m[1+E_m+\varepsilon_2\cos(\theta+\phi-\phi_2)] \text{ for } 180°\le\theta\le360° \quad (5)$$

where, Eccentricity at upper lobe,

$$\varepsilon_1=[{E_m}^2+\varepsilon^2-2E_m.\varepsilon.\cos(\phi)]^{1/2} \quad (6)$$

Eccentricity at lower lobe,

$$\varepsilon_2=[{E_m}^2+\varepsilon^2+2E_m.\varepsilon.\cos(\phi)]^{1/2} \quad (7)$$

$$\phi_1=\pi-\tan^{-1}\left[\frac{\phi}{E_m-\varepsilon.\cos\phi}\right] \quad (8)$$

$$\phi_2=\tan^{-1}\left[\frac{\phi}{E_m+\varepsilon.\cos\phi}\right] \quad (9)$$

Elliptical ratio,

$$E_m = \frac{C_h - C_m}{C_m} \tag{10}$$

The performance analysis for the elliptical bearing is evaluated based on its geometry.

Eccentricity ratio, attitude angle, Sommerfeld number are calculated for upper and lower lobe to evaluate the performance parameters mentioned in the Eqs. (6-9). However, for an elliptical bearing, the values are selected for the lower lobe region due to a loaded segment of bearing [2]. The geometrical and operating parameters for bearings are enlisted in Table 1.

2.2 Dynamic Characteristics

The stiffness and damping coefficients are represented in a fluid film as shown in Fig. 3. A steady state position of the journal is established by the load W. The journal moves away from its equilibrium position due to the dynamic force like rotor unbalance force resulting in whirl phenomenon. The film dynamic forces are expressed as:

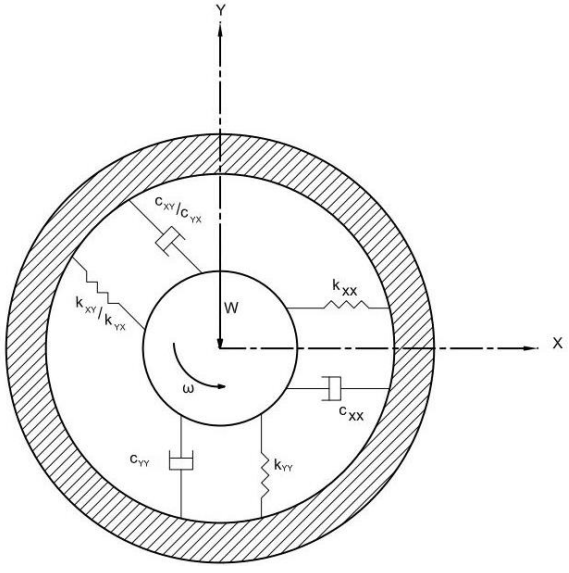

Fig. 3. Dynamic properties of fluid film.

$$\begin{Bmatrix} F_x \\ F_y \end{Bmatrix} = -\begin{bmatrix} k_{xx} & k_{xy} \\ k_{yx} & k_{yy} \end{bmatrix} \begin{Bmatrix} \Delta x \\ \Delta y \end{Bmatrix} - \begin{bmatrix} c_{xx} & c_{xy} \\ c_{yx} & c_{yy} \end{bmatrix} \begin{Bmatrix} \Delta \dot{x} \\ \Delta \dot{y} \end{Bmatrix} \tag{11}$$

The dimensionless bearing stiffness and damping coefficients are given by, $\bar{k}_{ij} = k_{ij}.c/W$, $\bar{c}_{ij} = c_{ij}.c/W$ and $i, j = x, y$ as a function of steady eccentricity ratio.

The linearized dimensionless stiffness and damping coefficients are given as [23],

$$\bar{k}_{XY} = \frac{\pi\left[\pi^2 - 2\pi^2\varepsilon^2 - \left(16 - \pi^2\right)\varepsilon^4\right]}{\varepsilon\sqrt{1-\varepsilon^2}}.Q(\varepsilon) \tag{12}$$

$$\bar{k}_{YX} = \frac{-\pi\left[\pi^2 + (32+\pi^2)\varepsilon^2 + 2\left(16 - \pi^2\right)\varepsilon^4\right]}{\varepsilon\sqrt{1-\varepsilon^2}}.Q(\varepsilon) \tag{13}$$

$$\bar{k}_{YY} = \frac{4\left[\pi^2 + (32+\pi^2)\varepsilon^2 + 2\left(16 - \pi^2\right)\varepsilon^4\right]}{(1-\varepsilon^2)}.Q(\varepsilon) \tag{14}$$

$$\bar{k}_{XX} = 4\left[2\pi^2 + \left(16 - \pi^2\right)\varepsilon^4\right].Q(\varepsilon) \tag{15}$$

$$\bar{c}_{XX} = \frac{2\pi\sqrt{(1-\varepsilon^2)}\left[\pi^2 + 2(\pi^2 - 8)\varepsilon^2\right]}{\varepsilon}.Q(\varepsilon) \tag{16}$$

$$\bar{c}_{YY} = \frac{2\pi\left[\pi^2 + 2(24 - \pi^2)\varepsilon^2 + \pi^2\varepsilon^4\right]}{\varepsilon\sqrt{(1-\varepsilon^2)}}.Q(\varepsilon) \tag{17}$$

$$\bar{c}_{XY} = \bar{c}_{YX} = -8\left[\pi^2 + 2(\pi^2 - 8)\varepsilon^2\right].Q(\varepsilon) \tag{18}$$

where,

$$Q(\varepsilon) = \frac{1}{\left[\pi^2\left(1-\varepsilon^2\right) + 16\varepsilon^2\right]^{1/2}} \tag{19}$$

2.3 Lubricant Selection

The Mobil DTE 20 series oils (DTE 24, DTE 25, and DTE 26) offers superior oxidation resistance. This property tends to extend the intervals for the replacement of oil and filter. In current days, the equipment manufacturers prefer these oils as they provide exceptional characteristics within a single product.

These oils find the applications where hydraulic system plays a vital role. These oils are used in the system where load carrying capacity is high and anti-wear protection as well as thin oil film protection is required. Based on these properties DTE 24, DTE 25 and DTE 26 oils are considered in this study to investigate the performance of journal bearing system [9,23]. The properties of lubricants are represented in Table 2. TiO_2 nanoparticles of size 40 nm are selected during the study to prepare nanolubricant. These nanoparticles have been added at 0.5 % weight of the lubricant sample. The selection, morphology, characterization of TiO_2 nanoparticles in the

lubricant and an impact of TiO_2 nanoparticles on the frictional and wear behaviour is represented in the author's previous work [9,23].

Table 2. Physico-Chemical Properties of lubricants considered in the study [23].

Lubricant properties	DTE 24	DTE 25	DTE 26
Viscosity, cSt @ 40°C (without nanoparticle)	32.42	46.33	67.43
Viscosity, cSt @ 40°C (with nanoparticle)	33.77	47.13	68.74
Pour Point, °C, ASTM D97	-27	-27	-21
Flash Point, COC, ASTM D92	220	232	236
Relative density/Specific gravity	0.869	0.877	0.885
Density, kg/m³	869	877	885
Specific heat at constant pressure, J/kgC	1951.0	1942.6	1934.3
Total acid number, mgKOH/gr. ASTM D 664	0.5767	0.5367	0.5271

The viscosity of nanolubricant is computed using a modified Krieger-Dougherty viscosity model [9,23].

3. EXPERIMENTAL TEST RIG

The detailed view of a journal bearing test rig is shown in Fig. 4a. The designed test rig mainly consists of a base frame, journal bearing assembly, loading system, belt drive, lubrication system, control, and measurement system. A base frame is prepared to mount all the components. This test rig is developed to fit all types of bearings viz. circular as well as non-circular geometry. The journal of 50 mm diameter is made up of EN8 grade driven by an electric motor. The journal is case hardened and cylindrical grinding is carried out on it. Phosphorous bronze material is selected for bearing and made to float on the journal. Twelve equidistant tapings of size ¼" BSP (6.35 mm) are provided on the peripheral surface of bearing as shown in Fig. 4b to locate the pressure and temperature measurement system. Each tap is located at 30° along the circumferential direction as shown in Fig. 5a. The circumferential location of sensor positions in the mid-plane of the bearing is represented in Fig. 5b. The sensors are mounted in each tap of a bearing to record the fluid film pressure and temperature. Inlet pressure and temperature of the oil is recorded at the start-up of each experimental trial. The journal is held between two pedestal bearings for stable operation and connected to the shaft of A.C. motor through the belt drive mechanism. The speed of a journal is controlled by a variable frequency drive (Make- Delta) in an anticlockwise direction that is connected to an electric motor. The speed of a journal can be reached up to 1000 r.p.m. that is viewed on speed indicator and is sensed by a proximity sensor. For experimental analysis, the speed of a journal is varied between 500 r.p.m. to 1000 r.p.m as mentioned in Table 1.

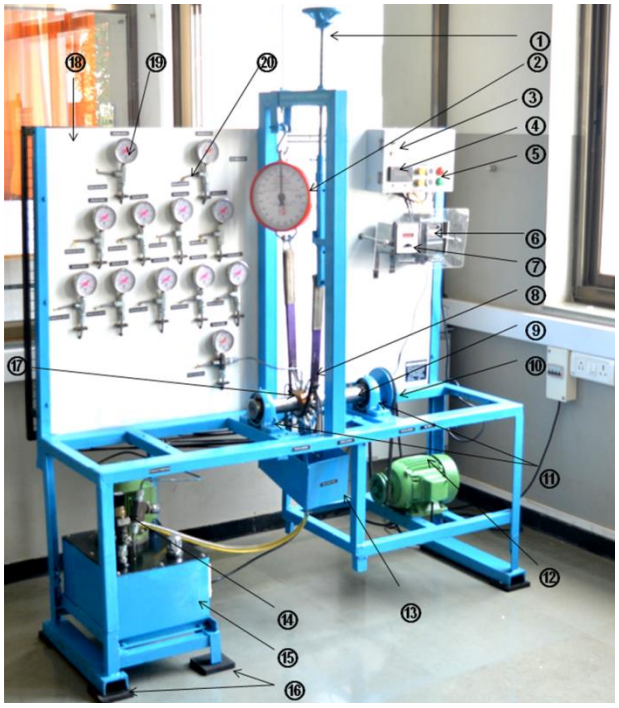

a)

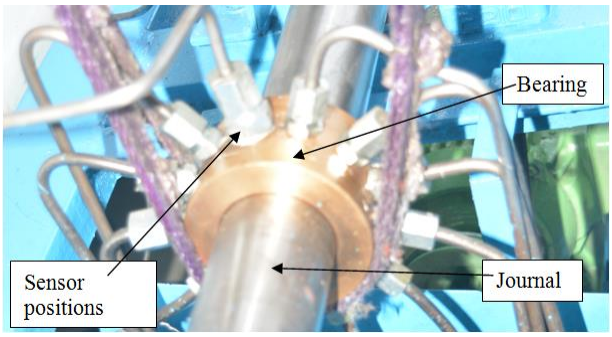

b)

Fig. 4. a) Journal bearing test rig: 1. Loading lever 2. Dial spring balance 3. Toggle switches 4. Speed indicator 5. Mains ON/OFF indicator 6. Variable frequency drive 7. Multipoint temperature indicator 8. Belt 9. Journal 10. Belt drive 11. Support bearings 12. Motor 13. Side leakage collector tank 14. Pressure relief valve 15. Lubrication system 16. Anti-vibration pads 17. Bearing 18. Frame 19. Pressure gauges (12 no.s) 20. Temperature sensors (12 no.s); b) Closed view of journal bearing assembly.

The pressurized lubrication is provided through a hydraulic power pack. The capacity of the motor (0.5 h.p.) in the lubrication system is selected based on the oil flow through the system. The selected grade of lubricant is passed through the power pack with 0.4 MPa internal pressure and 25 °C inlet temperature to a maximum 10 % deviation due to atmospheric conditions for all the experiments. The lubricant is collected inside the side leakage tank through side flow and recirculated during the experiments. The loading arrangement on the journal bearing is given through the dial type spring balance and belt (1000 kg capacity).

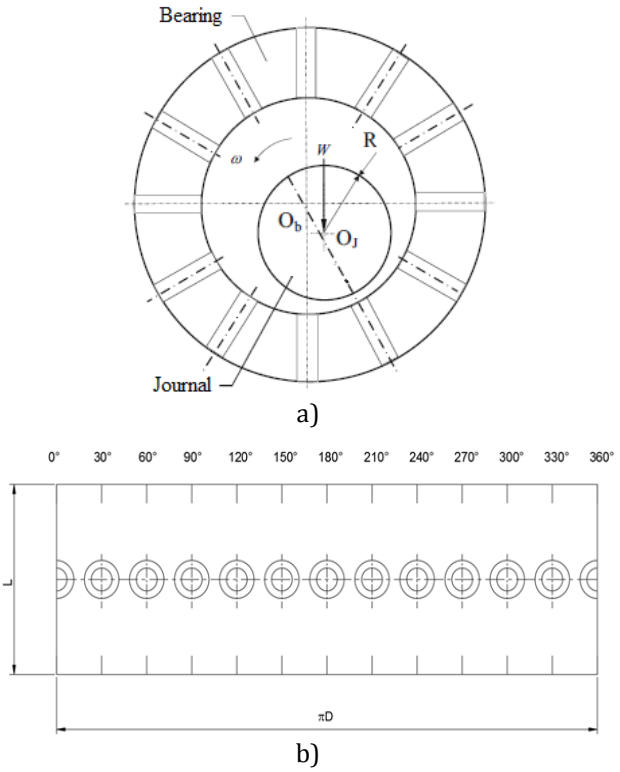

Fig. 5. Schematic view of journal bearing: a) Angular location of pressure and temperature sensors; b) Circumferential view of bearing surface.

The load can be varied from 0 to 2 kN that is given through the lever mechanism. The oil flow is provided in the system that is controlled by a flow control valve. The pressure generated in the fluid film along the circumference of the bearing is measured with the help of glycerine filled pressure gauges (Make-Fiebig, 0-3000 psi). In a similar way, the temperature along the circumferential points is measured using K type thermocouples (Make-Honeywell, 0-600 °C) that are indicated on multipoint temperature indicator at various positions. Anti-vibration pads are provided at the base of a frame to reduce the vibration transmitted to the foundation. The measurement parameters are noted after half an hour operation of the system as it attains a steady state condition [2]. The pressure gauges on journal bearing test rig are calibrated as per IS 3624 against the master gauge and accuracy found within the limit ±1% with maximum error 0.38 %. The uncertainty of measurement is recorded as ±0.74 % (95 % confidence level) of reading. Thermocouples are also calibrated as per IS 2054-1962 against master K type thermocouple with setpoint temperatures 50 °C, 100 °C, 150 °C with expanded uncertainty ±0.80 °C (95.45 % confidence level) and obtained readings are found within the standard error ±4.50 °C.

4. RESULTS AND DISCUSSION

Three sets of readings are taken for each operating condition to get the desired accuracy and the mean reading is considered for analysis. The inlet pressure and inlet temperature readings are noted at the initial phase of each run after applying the load through a lever mechanism. After enriching a steady state, the film pressure and temperature readings along the periphery of a journal bearing are noted down. The pressure ratio and temperature rise in a fluid film are computed after the experimental trials and following plots (Figs. 6-7) have been obtained.

The values of $\left(\frac{p}{p_{\max}}\right)$ ratio are taken from Raimondi-Boyd chart for the comparative analysis.

The intermediate values of the pressure ratio for the eccentricity ratio are computed using a linear interpolation method. The maximum pressure reading has been identified during the test and pressure ratio is computed which is compared with the theoretical pressure ratio as shown in Fig. 6. The average pressure p is computed and a ratio $(p/p_{max.})$ has been obtained for all the cases as shown in Table 3. Theoretical pressure distribution is computed and represented in the author's previous work [9]. The analytical results of the pressure ratio are validated experimentally in this work. The pressure ratio decreases significantly in an elliptical journal bearing that indicates the rise in maximum pressure distribution. As the viscosity of the lubricant increases from Mobil

DTE 24 to Mobil DTE 26 the pressure ratio increases. The readings of pressure in a fluid film for the bearing configurations have been noted down at the steady condition. For an elliptical bearing, the pressure ratio is almost constant as 0.46 at the unloaded upper lobe as eccentricity ratio remains the same. However, the pressure ratio gets changed at the loaded lower lobe significantly due to variation in eccentricity ratio. As seen from the Fig. 6a and Table 3, when an elliptical bearing is operating with Mobil DTE 24 lubricating oil without TiO_2 nanoparticle additives, the pressure distribution rises in the range of -2.73 % to 78.78 % as compared to the pressure distribution in the plain bearing running in the speed range of 500 to 1000 r.p.m. Similarly, the pressure distribution in an elliptical bearing rises over the pressure distribution in a plain bearing in the range of 19.45 % to 182.69 % for Mobil DTE 25 oil without TiO_2 nanoparticle additives and in the range of 91.89 % to 351.01 % for Mobil DTE 26 oil without TiO_2 nanoparticle additives for same operating conditions. A similar procedure has been adapted for the comparative analysis of pressure ratio in both plain and elliptical journal bearings operating with the selected grades of the lubricating oils that contains TiO_2 nanoparticle additives. Fig. 6b depicts the comparison of pressure distribution in the journal bearing for a wide range of operating conditions. When an elliptical bearing is operating with Mobil DTE 24 oil with TiO_2 nanoparticle additives, the pressure distribution rises in the range of -2.48 % to 87.79 % over the pressure distribution in the plain bearing running in the speed range of 500 to 1000 r.p.m. Similarly, the pressure distribution in an elliptical bearing rises over the pressure distribution in a plain bearing in the range of 21.9 % to 187.12 % for Mobil DTE 25 oil without TiO_2 nanoparticle additives and in the range of 96.68 % to 364.34 % for Mobil DTE 26 oil with TiO_2 nanoparticle additives for same operating conditions. This indicates the increase in pressure distribution in the oil film when it contains TiO_2 nanoparticle additives in the lubricating oils.

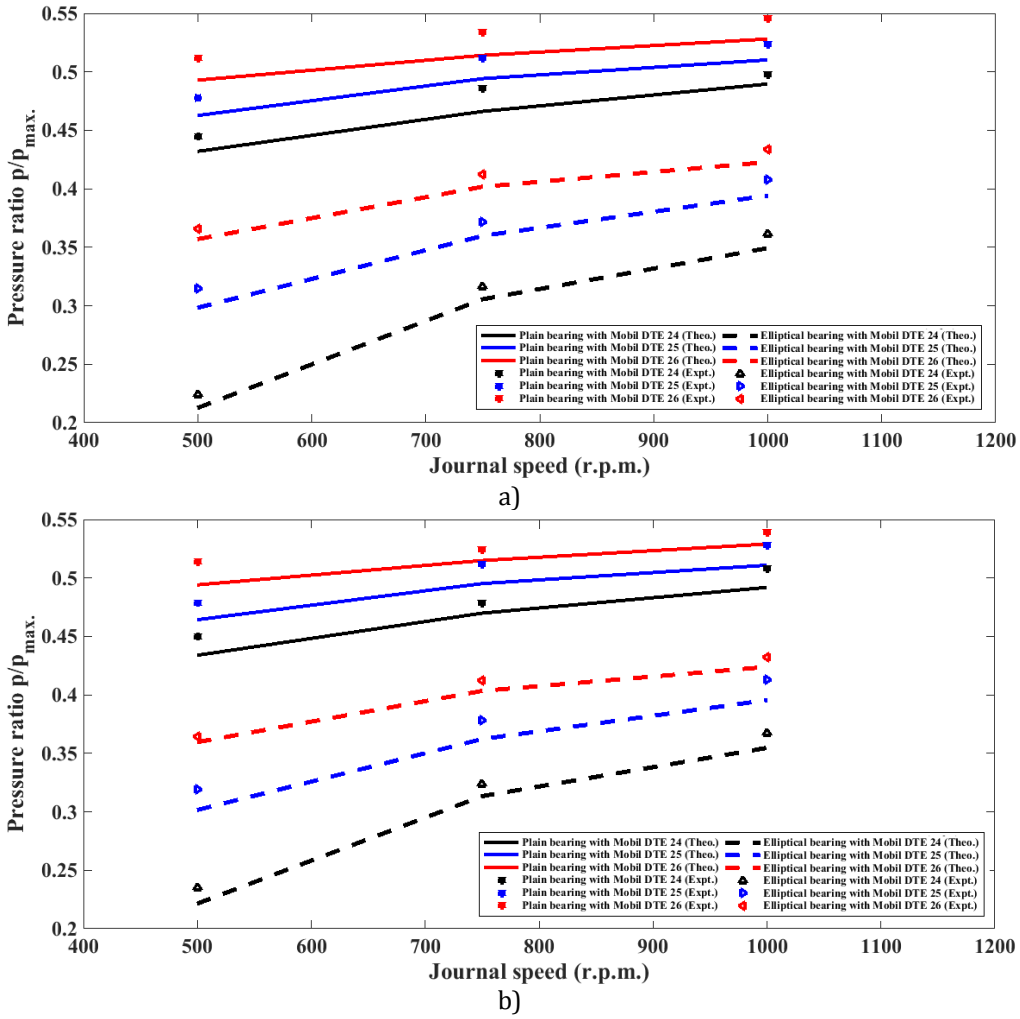

a)

b)

Fig. 6. Comparison of pressure ratio for different lubricants at various speeds: a) without NP; b) with NP.

Table 3. Comparison between experimental and analytical data for performance analysis at different operating speeds.

Type of bearing	Type of lubricant	Speed (r.p.m.)	ε	p/p_{max} (Theo.)	p/p_{max} (Expt.)	% Error	p_{max} (Theo.)	p_{max} (Expt.)	ΔT (Theo.)	ΔT (Expt.)	% Error
Plain bearing without TiO_2	Mobil DTE 24	500	0.5506	0.432	0.4449	2.986	1.5622	1.5169	4.418	4.12	6.745
		750	0.4517	0.4662	0.4862	4.29	1.6538	1.5859	5.733	5.12	10.69
		1000	0.375	0.4896	0.4981	1.736	1.6836	1.6548	7.341	7.145	2.67
	Mobil DTE 25	500	0.4616	0.4627	0.478	3.307	1.6144	1.5629	5.6058	5.45	2.779
		750	0.3547	0.4942	0.512	3.602	1.6996	1.6433	8.0936	7.947	1.811
		1000	0.2835	0.5102	0.524	2.705	1.7241	1.6778	10.705	9.895	7.567
	Mobil DTE 26	500	0.3603	0.4929	0.512	3.875	1.6469	1.5859	7.8828	7.612	3.435
		750	0.2663	0.5141	0.534	3.871	1.7415	1.6778	11.3378	10.895	3.905
		1000	0.2041	0.5281	0.545	3.2	1.7765	1.7238	13.6068	12.657	6.98
Plain bearing with TiO_2	Mobil DTE 24	500	0.5451	0.4339	0.45	3.711	1.5554	1.5169	4.4876	4.2597	5.078
		750	0.4409	0.4699	0.479	1.937	1.663	1.6318	5.8755	5.5547	5.46
		1000	0.3647	0.4919	0.508	3.273	1.7331	1.6778	7.724	6.9758	9.687
	Mobil DTE 25	500	0.4572	0.4643	0.4786	3.08	1.6336	1.5859	5.66	5.3891	4.786
		750	0.35	0.4952	0.5118	3.352	1.711	1.6548	8.2672	8.245	0.268
		1000	0.2806	0.5109	0.5285	3.445	1.7586	1.7008	10.8146	10.4856	3.042
	Mobil DTE 26	500	0.3551	0.4941	0.5145	4.129	1.7105	1.6433	8.0791	7.647	5.348
		750	0.2626	0.5149	0.5245	1.864	1.7206	1.6893	11.4725	11.245	1.983
		1000	0.1997	0.529	0.539	1.89	1.8031	1.7697	13.7722	13.457	2.288
Elliptical bearing without TiO_2	Mobil DTE 24	500	0.9254	0.2127	0.224	5.313	1.8948	1.8272	1.2114	1.154	4.738
		750	0.8112	0.3056	0.316	3.403	1.9124	1.8501	2.0287	1.987	2.055
		1000	0.7289	0.3493	0.361	3.35	1.9551	1.8961	2.71	2.6947	0.564
	Mobil DTE 25	500	0.8223	0.2983	0.3145	5.431	1.9592	1.8616	1.9479	1.854	4.821
		750	0.7083	0.3598	0.372	3.391	1.9696	1.8961	2.8783	2.6547	7.768
		1000	0.6409	0.3942	0.408	3.501	1.9872	1.9191	3.4205	3.3397	2.362
	Mobil DTE 26	500	0.7139	0.357	0.366	2.521	1.9206	1.8731	2.8324	2.754	2.768
		750	0.626	0.4018	0.412	2.539	1.9544	1.9076	3.5371	3.4578	2.242
		1000	0.5773	0.4228	0.434	2.649	1.9841	1.9306	4.0523	4.1245	1.781
Elliptical bearing with TiO_2	Mobil DTE 24	500	0.9188	0.2215	0.235	6.095	1.9395	1.8961	1.1845	1.198	1.139
		750	0.7992	0.3134	0.3234	3.191	1.9591	1.9076	2.1166	2.086	1.445
		1000	0.7183	0.3547	0.367	3.468	1.9855	1.9191	2.7965	2.7585	1.358
	Mobil DTE 25	500	0.8174	0.3016	0.319	5.769	1.9704	1.8976	1.9835	1.857	6.378
		750	0.7036	0.3622	0.378	4.362	1.9935	1.9376	2.9166	2.8564	2.064
		1000	0.6383	0.3955	0.413	4.425	2.0145	1.9506	3.4403	3.404	1.055
	Mobil DTE 26	500	0.7087	0.3596	0.364	1.224	1.9421	1.9157	2.8749	2.7598	4.004
		750	0.6228	0.4034	0.412	2.132	1.9776	1.9346	3.5623	3.4598	2.877
		1000	0.5742	0.4239	0.432	1.911	1.2064	1.9891	4.0946	4.0598	0.849

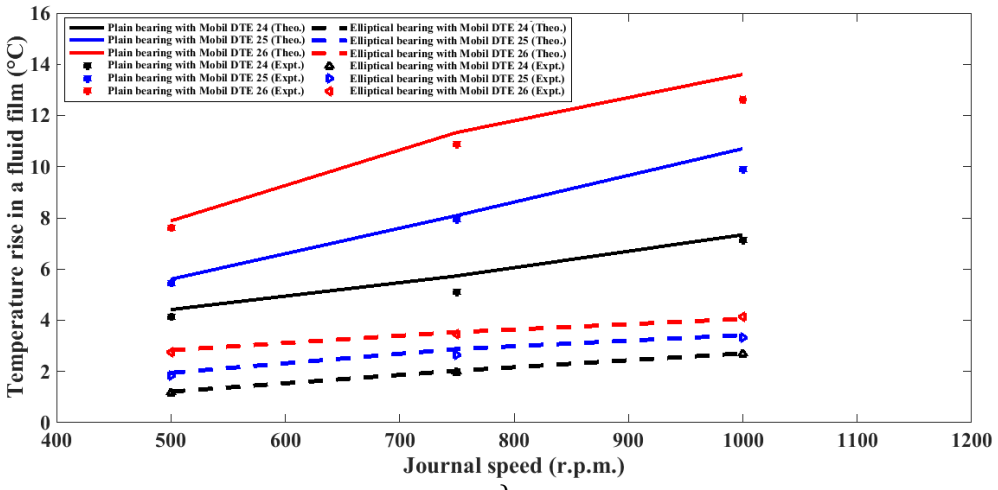

a)

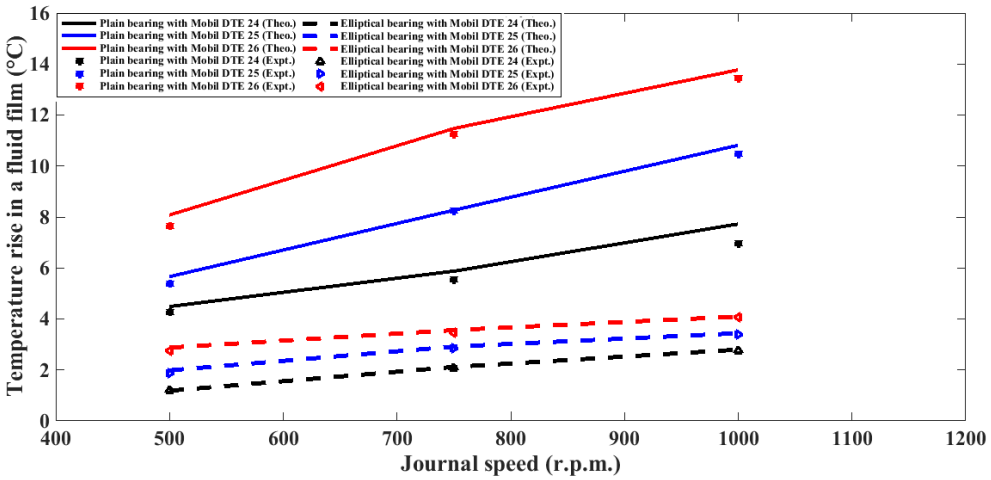

b)

Fig. 7. Comparison of temperature rise in a fluid film for different lubricants at various speeds: a) without NP; b) with NP.

A good agreement between the theoretical pressure ratio and experimental pressure ratio is observed for all three grades of lubricant that represents the validation of the author's theoretical work. The maximum 5.43 % of error is found between the theoretical and experimental pressure ratio during the analysis as shown in Table 3. However, the minor difference is observed in the experimental pressure readings due to the losses in the piping. Similarly, the temperature readings have been observed during an each trial for both the bearing configurations. Fig. 7a represents the comparative analysis of an experimental and theoretical temperature rise in the fluid film for plain as well as elliptical bearings operating with various conditions. Three grades of lubricating oils have been considered here without TiO_2 nanoparticle additives. It has been observed that when an elliptical bearing is operating with Mobil DTE 24 oil without TiO_2 nanoparticle additives, the temperature rise in the oil film decreases in the range of 63.08 % to 72.58 % as compared to the temperature rise in the plain bearing running in the speed range of 500 to 1000 r.p.m. Similarly, when the bearings were operated with Mobil DTE 25 oil without TiO_2 nanoparticle additives, the temperature rise is reduced in the range of 64.43 % to 68.04 % in the elliptical bearing while in the case of Mobil DTE 26 oil without TiO_2 nanoparticle additives, the temperature rise is reduced in the range of 64.06 % to 70.21 % in the elliptical bearing as compared to the plain bearing.

The similar procedure is adopted for the comparative analysis of an experimental and theoretical temperature rise in the fluid film of lubricating oil containing TiO_2 nanoparticle additives. The Fig. 7b depicts the comparative analysis of an experimental and theoretical temperature rise in the fluid film for the plain as well as elliptical bearings operating with TiO_2 nanoparticle additives in the lubricating oils. It has been observed that the elliptical bearing when operating with Mobil DTE 24 oil with TiO_2 nanoparticle additives causes to decrease the temperature rise in the fluid film in the range of 63.79 % to 73.60 % as compared to the temperature profile in the plain journal bearing. The temperature rise is reduced in the range of 64.72 % to 68.18 % for Mobil DTE 25 oil with TiO_2 nanoparticle additives and 64.41 % to 70.26 % for Mobil DTE 26 oil TiO_2 nanoparticle additives respectively in the elliptical journal bearing over the plain journal bearing between the speed range 500 to 1000 r.p.m. A comparison between the theoretical and experimental temperature rise in the fluid film is carried out as shown in Fig. 7. The theoretical temperature rise has been considered from the author's previous work [9]. During an experimental procedure, the inlet temperature has been noted at the starting phase of each run and temperature readings at the outlet tapings have been noted simultaneously with pressure readings. An average temperature reading is considered for all the outlet temperature readings and the temperature rise in a fluid film is computed as shown in Table 3. A mean temperature rise obtained after three sets of readings is then compared with the theoretical temperature rise and found to be very close to each other as depicted in Fig. 7. The minor difference is observed due to the piping losses as

well as the effect of atmospheric conditions. It is very remarkable to mention that the temperature rise is very low for an elliptical bearing configuration than that of a plain bearing through the experimental methodology also. It is very desirable as far as the performance of the system is concerned. The maximum 10.7 % of error has been found between the theoretical and experimental temperature rise in a fluid film during the analysis. The Figs. 8-9 represent the variation in the dynamic properties (stiffness and damping) of the fluid film journal bearing. The stiffness and damping characteristics have been evaluated after the addition of TiO_2 nanoparticles in the lubricant. The dynamic characteristics such as stiffness and damping properties are measured for both the bearings (plain and elliptical) as per Eqs. (12-19) at various operating conditions.

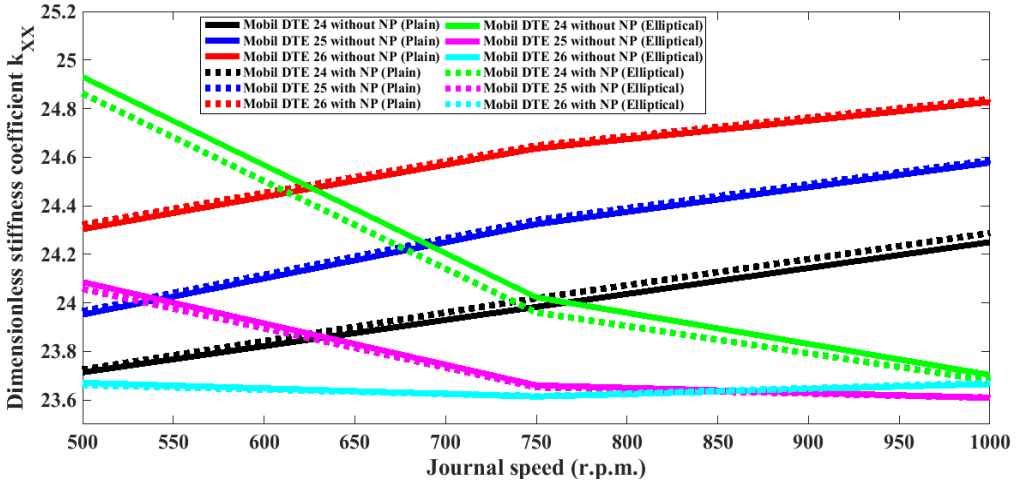

a)

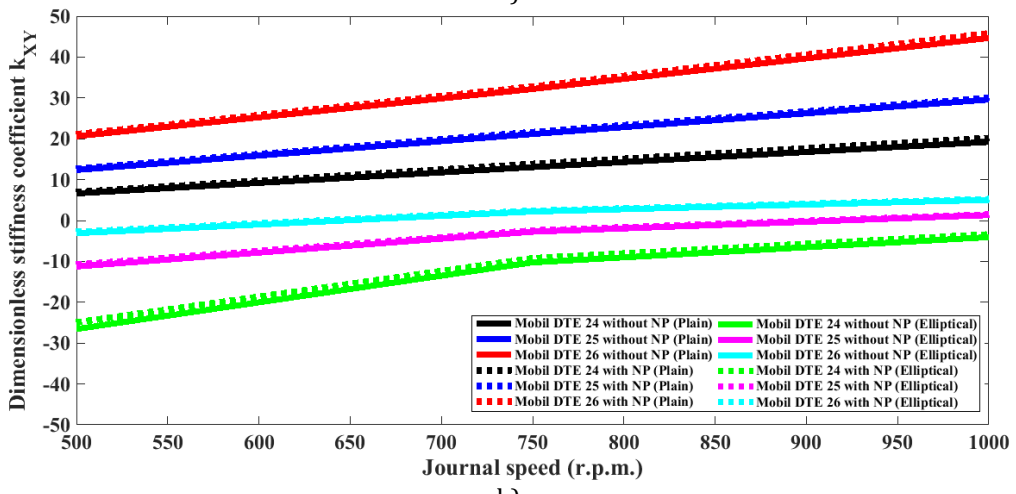

b)

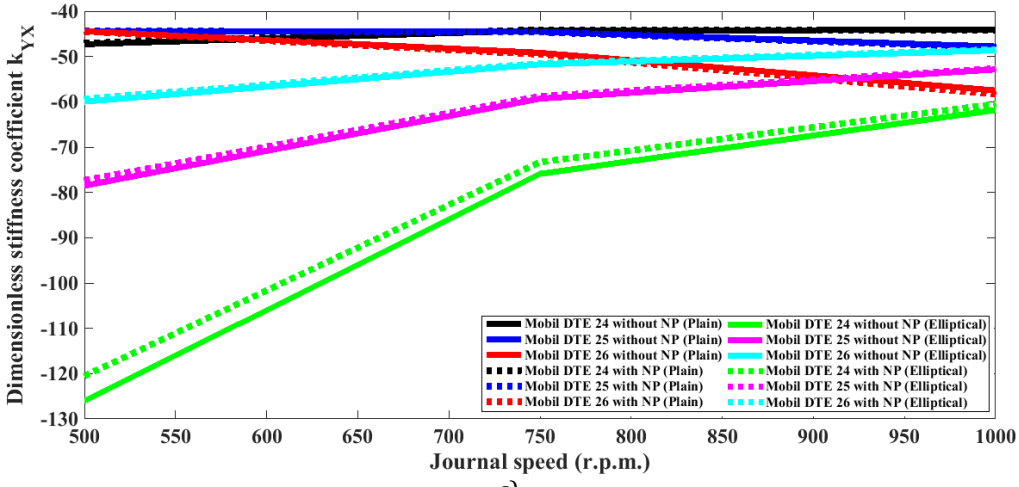

c)

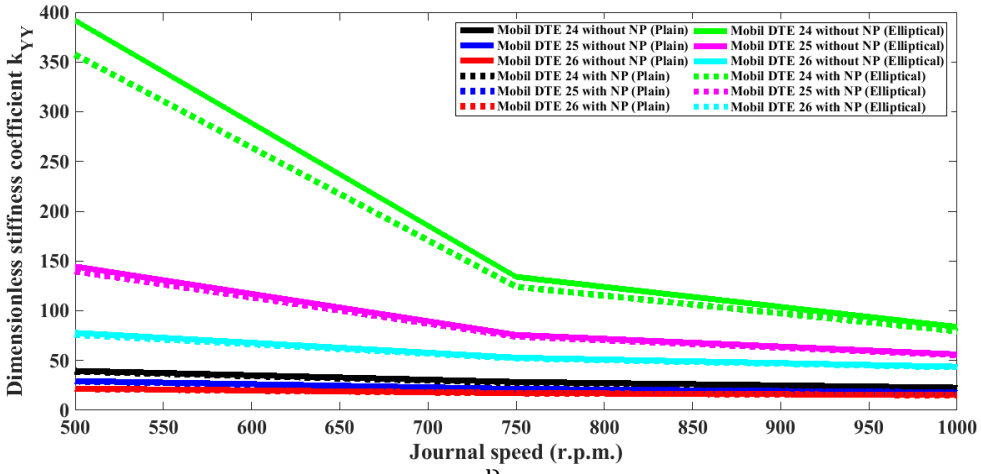

Fig. 8. Variation in dimensionless stiffness coefficients with and without NP (TiO_2) in the lubricant: a) k_{XX} ; b) k_{XY} ; c) k_{YX} and d) k_{YY} .

Table 4. Dynamic properties for journal bearing at different operating speeds.

Type of bearing	Type of lubricant	Speed (r.p.m.)	ε	$Q(\varepsilon)$	$\bar{k}_{XY}$	$\bar{k}_{YX}$	$\bar{k}_{YY}$	$\bar{k}_{XX}$	$\bar{c}_{XX}$	$\bar{c}_{YY}$	$\bar{c}_{XY}/\bar{c}_{YX}$
Plain bearing without TiO_2	Mobil DTE 24	500	0.5506	0.292	6.630	-47.282	39.708	23.714	30.607	77.217	-25.704
		750	0.4517	0.300	13.061	-44.236	28.516	23.983	39.569	75.025	-25.507
		1000	0.375	0.305	19.235	-44.138	22.733	24.250	49.289	77.457	-25.386
	Mobil DTE 25	500	0.4616	0.299	12.359	-44.402	29.418	23.951	38.526	74.997	-25.525
		750	0.3547	0.307	21.168	-44.522	21.505	24.324	52.499	78.881	-25.358
		1000	0.2835	0.311	29.592	-47.794	17.990	24.577	67.148	87.624	-25.275
	Mobil DTE 26	500	0.3603	0.306	20.618	-44.396	21.833	24.303	51.580	78.449	-25.366
		750	0.2663	0.312	32.176	-49.187	17.302	24.635	71.803	90.922	-25.258
		1000	0.2041	0.314	44.654	-57.493	15.262	24.827	94.951	109.343	-25.205
Plain bearing with TiO_2	Mobil DTE 24	500	0.5451	0.292	6.963	-47.032	38.935	23.725	31.034	76.956	-25.691
		750	0.4409	0.301	13.846	-44.092	27.577	24.019	40.753	75.124	-25.489
		1000	0.3647	0.306	20.196	-44.308	22.096	24.288	50.876	78.131	-25.372
	Mobil DTE 25	500	0.4572	0.299	12.669	-44.324	29.012	23.966	38.985	75.002	-25.517
		750	0.35	0.307	21.639	-44.641	21.237	24.341	53.292	79.267	-25.352
		1000	0.2806	0.311	30.009	-48.008	17.870	24.587	67.894	88.140	-25.272
	Mobil DTE 26	500	0.3551	0.307	21.128	-44.513	21.529	24.322	52.433	78.849	-25.359
		750	0.2626	0.312	32.770	-49.527	17.162	24.648	72.881	91.712	-25.254
		1000	0.1997	0.314	45.802	-58.353	15.142	24.839	97.121	111.187	-25.202
Elliptical bearing without TiO_2	Mobil DTE 24	500	0.92538	0.257	-26.556	-126.030	391.742	24.931	8.652	190.294	-26.894
		750	0.81121	0.268	-10.257	-75.898	134.062	24.023	14.977	116.306	-26.454
		1000	0.72887	0.276	-4.078	-61.813	83.786	23.703	19.314	96.156	-26.179
	Mobil DTE 25	500	0.82228	0.267	-11.262	-78.522	144.461	24.086	14.401	120.119	-26.494
		750	0.70825	0.278	-2.750	-59.302	75.752	23.660	20.445	92.660	-26.116
		1000	0.64089	0.284	1.320	-52.862	56.194	23.609	24.387	83.977	-25.924
	Mobil DTE 26	500	0.71389	0.277	-3.107	-59.958	77.827	23.671	20.133	93.569	-26.133
		750	0.62596	0.285	2.193	-51.729	52.867	23.614	25.328	82.517	-25.885
		1000	0.57733	0.290	5.038	-48.634	43.784	23.665	28.619	78.725	-25.765
Elliptical bearing with TiO_2	Mobil DTE 24	500	0.91884	0.258	-24.940	-120.530	357.305	24.862	9.063	182.108	-26.867
		750	0.79924	0.269	-9.232	-73.310	124.127	23.961	15.599	112.556	-26.412
		1000	0.71834	0.277	-3.393	-60.493	79.529	23.680	19.888	94.312	-26.147
	Mobil DTE 25	500	0.81735	0.268	-10.807	-77.324	139.670	24.057	14.658	118.376	-26.476
		750	0.70356	0.278	-2.455	-58.771	74.086	23.653	20.706	91.927	-26.102
		1000	0.63834	0.284	1.470	-52.661	55.603	23.609	24.547	83.717	-25.918
	Mobil DTE 26	500	0.70866	0.278	-2.775	-59.348	75.897	23.661	20.423	92.724	-26.117
		750	0.62283	0.286	2.376	-51.503	52.204	23.616	25.529	82.229	-25.877
		1000	0.57425	0.290	5.220	-48.466	43.284	23.670	28.841	78.531	-25.758

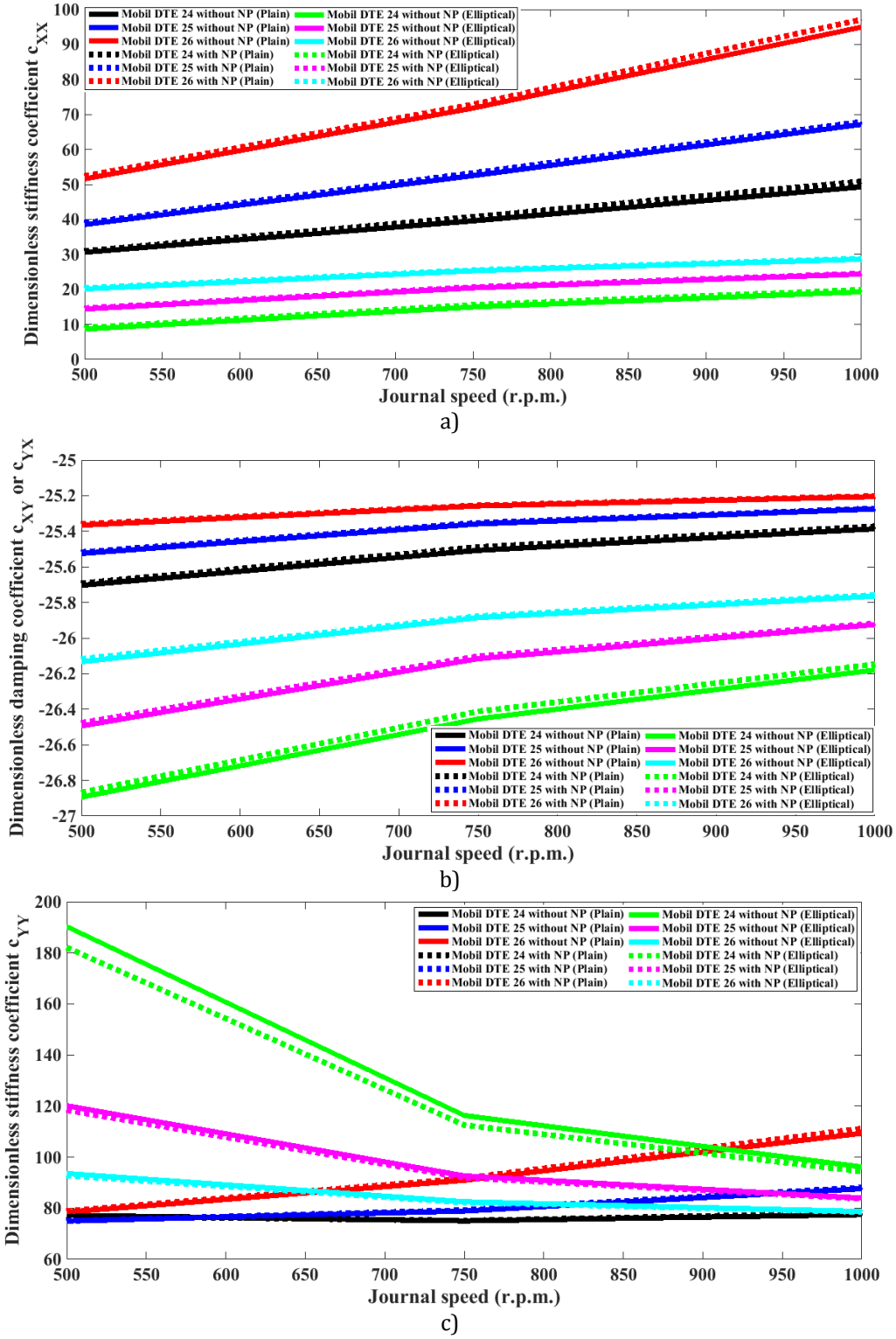

Fig. 9. Variation in dimensionless damping coefficients with and without NP (TiO_2) in the lubricant: a) c_{XX}; b) c_{XY} or c_{YX}; and c) c_{YY}.

These dynamic characteristics are depending on the eccentricity ratio. Hence, by considering the relevant eccentricity ratio, the dynamic properties have been evaluated as shown in Table 4. However, for an elliptical journal bearing, the eccentricity ratio in the loaded lobe has been considered in the analysis as the eccentricity ratio in the unloaded lobe remains the same (ε_1=0.5). It has observed that after the addition of TiO_2 nanoparticles in the lubricating oil, the dimensionless damping coefficients ($\bar{c}_{XX}$, $\bar{c}_{XY}$,

$\bar{c}_{YX}$, $\bar{c}_{YY}$) and dimensionless stiffness coefficients ($\bar{k}_{XY}$, $\bar{k}_{YX}$) increases whereas dimensionless stiffness coefficients ($\bar{k}_{XX}$, $\bar{k}_{YY}$) decreases for a plain as well as an elliptical bearing. It is also found that in an elliptical bearing the dimensionless stiffness coefficients ($\bar{k}_{XX}$, $\bar{k}_{YY}$) and dimensionless damping coefficient ($\bar{c}_{YY}$) increases significantly while other remaining dimensionless coefficients decreases due to an increase in the eccentricity ratio between *X-Y* and *Y-X* regions. It is also noted that in *X-Y* and *Y-X* region the plain bearing shows superior dynamic performance with an increase in speed. TiO_2 nanoparticle additives influence the dynamic properties of the bearing that helps to improve the performance of the journal bearing system. Table 4 and Fig. 8a represents the comparison of dimensionless stiffness coefficient k_{XX} in plain as well as elliptical journal bearings operating with a wide range of operating conditions. Due to the addition of TiO_2 nanoparticles in the lubricants, the dimensionless stiffness coefficient k_{XX} increases in the range of 0.02 % to 0.27 %. Similarly, Figs. 8b, 8c and 8d provides the comparison of dimensionless stiffness coefficients k_{XY}, k_{YX} and k_{YY} respectively in plain as well as elliptical journal bearings. The dimensionless stiffness coefficients k_{XY} increased in the range of 1.84 % to 16.80 %, k_{YX} increased in the range of 0.17 % to 4.36% and k_{YY} decreased upto 8.79 %.

The Fig. 9 depicts the dimensionless damping coefficients in all the directions of journal bearings operating with various operating conditions. The Figs. 9a, 9b and 9c indicates the comparison of dimensionless damping coefficients c_{XX}, c_{XY} or c_{YX} and c_{YY} respectively. As seen in Table 4 and Fig. 9, the dimensionless damping coefficients c_{XX} increases in the range of 0.77 % to 4.74 %, c_{XY} or c_{YX} increases in the range of 0.02% to 0.16% and c_{YY} decreases upto 4.30 %. The dimensionless stiffness coefficients k_{YY} and c_{YY} have been reduced in both journal bearings as the pressure of the lubricating oil is constant in the direction of oil film thickness. Hence, the pressure gradient becomes zero in Y-Y direction and dynamic characteristics are considered as negligible in this region.

5. CONCLUSION

The plain and elliptical journal bearings operating with TiO_2 nanoparticle based lubricants have been considered in this research study. An experimental approach has presented to evaluate the performance characteristics at different operating conditions. TiO_2 nanoparticles (0.5 %wt.) have been added in the lubricants to analyze the performance of the bearings. The static and dynamic performance characteristics of a plain as well as an elliptical journal bearing have been evaluated and presented in this paper.

The selected lubricants are implemented in the developed journal bearing test rig and rigorous experimentation is carried out on the test rig to validate the analytical results. The obtained experimental findings are in a very good agreement with the analytical results. The following conclusions have been drawn from the present study:

- The bearing geometry plays a crucial role to analyze the performance of fluid film lubricated journal bearing. The static performance characteristics have been improved using an elliptical journal bearing over a plain journal bearing. The pressure distribution increases upto 78.78%, 182.69 % and 351.01 % in an elliptical bearing as compared to a plain bearing when operating with Mobil DTE 24, Mobil DTE 25 and Mobil DTE 26 respectively. Also in an elliptical bearing, the temperature rise decreases upto 72.58 %, 68.04 % and 70.21 % when it was operating with Mobil DTE 24, Mobil DTE 25 and Mobil DTE 26 lubricating oil respectively.
- The performance characteristics are also improved using TiO_2 nanoparticle additives in the lubricating oils for both plain and elliptical journal bearings. After addition of TiO_2 nanoparticle additives, the pressure distribution increases upto 87.79 %, 187.12 % and 364.34 % in an elliptical bearing as compared to a plain bearing when operating with Mobil DTE 24, Mobil DTE 25 and Mobil DTE 26 respectively. At the same time, the temperature rise in an elliptical bearing

operating with Mobil DTE 24, Mobil DTE 25 and Mobil DTE 26 containing TiO_2 nanoparticle reduces upto 73.60 %, 68.18 % and 70.26 % respectively.

- Experimental findings for pressure ratio and temperature rise in a fluid film are compared with the analytical results and found very near to each other. An elliptical bearing operating with TiO_2 nanoparticle based nanolubricant shows superior performance over other combinations.
- TiO_2 nanoparticle additives influence the dynamic properties such as stiffness and damping of the bearing that helps to improve the performance of the journal bearing system. The stiffness and damping properties of the oil film are improved with the addition of TiO_2 nanoparticles in the lubricant. The dimensionless stiffness coefficients $\bar{k}_{XY}$, $\bar{k}_{YX}$ and $\bar{k}_{XX}$ are increased upto 16.80%, 4.36% and 0.27% respectively while $\bar{k}_{YY}$ has been decreased upto 8.79%. The dimensionless damping coefficients $\bar{c}_{XY}$ / $\bar{c}_{YX}$ and $\bar{c}_{XX}$ are increased upto 0.12% and 4.74% respectively whereas $\bar{c}_{YY}$ decreases by 4.30 %.

REFERENCES

[1] F.P. Brito, A.S. Miranda, J.C.P. Claro, M. Fillon, *Experimental comparison of the performance of a journal bearing with a single and a twin axial groove configuration*, Tribology International, vol. 54, pp. 1–8, 2012, doi: 10.1016/j.triboint.2012.04.026

[2] D.Y. Dhande, D.W. Pande, *Multiphase flow analysis of hydrodynamic journal bearing using CFD coupled Fluid Structure Interaction considering cavitation*, Journal of King Saud University-Engineering Sciences, vol. 30, iss. 4, pp. 345-354, 2018, doi: 10.1016/j.jksues.2016.09.001

[3] A.F. Cristea, J. Bouyer, M. Fillon, M.D. Pascovici, *Transient Pressure and Temperature Field Measurements in a Lightly Loaded Circumferential Groove Journal Bearing from Startup to Steady-State Thermal Stabilization*, Tribology Transactions, vol. 60, iss. 6, pp. 988-1010, 2017, doi: 10.1080/10402004.2016.1241330

[4] P.C. Mishra, R.K. Pandey, K. Athre, *Temperature profile of an elliptic bore journal bearing*, Tribology International, vol. 40, iss. 3, pp. 453–458, 2007, doi: 10.1016/j.triboint.2006.04.009

[5] R. Sehgal, *Experimental Measurement of Oil Film Temperatures of Elliptical Journal Bearing Profile Using Different Grade Oils*, Tribology Online, vol. 5, iss. 6, pp. 291–299, 2010, doi: 10.2474/trol.5.291

[6] K.G. Binu, K. Yathish, R. Mallya, B.S. Shenoy, D.S. Rao, R. Pai, *Experimental study of hydrodynamic pressure distribution in oil lubricated two-axial groove journal bearing*, Materials Today: Proceedings, vol. 2, iss. 4-5, pp. 3453–3462, 2015, doi: 10.1016/j.matpr.2015.07.321

[7] M. Kasai, M. Fillon, J. Bouyer, S. Jarny, *Influence of lubricants on plain bearing performance: Evaluation of bearing performance with polymer-containing oils*, Tribology International, vol. 46, iss. 1, pp. 190-199, 2012, doi: 10.1016/j.triboint.2011.03.009

[8] A.F. Cristea, J. Bouyer, M. Fillon, M.D. Pascovici, *Pressure and Temperature Field Measurements of a Lightly Loaded Circumferential Groove Journal Bearing*, Tribology Transactions, vol. 54, iss. 5, pp. 806-823, 2011, doi: 10.1080/10402004.2011.604758

[9] S.R. Suryawanshi, J.T. Pattiwar, *Effect of TiO_2 Nanoparticles Blended with Lubricating Oil on the Tribological Performance of the Journal Bearing*, Tribology in Industry, vol. 40, no. 3, pp. 370-391, 2018, doi: 10.24874/ti.2018.40.03.04

[10] K.G. Binu, B.S. Shenoy, D.S. Rao, R. Pai, *A Variable Viscosity Approach for the Evaluation of Load Carrying Capacity of Oil Lubricated Journal Bearing with TiO_2 Nanoparticles as Lubricant Additives*, Procedia Materials Science, vol. 6, pp. 1051–1067, 2014, doi: 10.1016/j.mspro.2014.07.176

[11] S. Baskar, G. Sriram, *Tribological behavior of journal bearing material under different lubricants*, Tribology in Industry, vol. 36, no. 2, pp. 127–133, 2014.

[12] X. Li, M. Murashima, N. Umehara, *Effect of nanoparticles as lubricant additives on friction and wear behavior of tetrahedral amorphous carbon (ta-C) coating*, Jurnal Tribologi, vol. 16, pp. 15-29, 2018.

[13] B. Bongfa, P.A. Atabor, A. Barnabas, M.O. Adeoti, *Comparison of lubricant properties of Castor oil and commercial engine oil*, Jurnal Tribologi, vol. 5, pp. 1-10, 2015.

[14] W. Gunnuang, C. Aiumpornsin, M. Mongkolwongrojn, *Effect of Nanoparticle Additives on Journal Bearing Lubricated with Non-Newtonian Carreau Fluid*, Applied Mechanics and Materials, vol. 751, pp. 137-142, 2015, doi: 10.4028/www.scientific.net/AMM.751.137

[15] A.A. Solghar, *Investigation of nanoparticle additive impacts on thermohydrodynamic characteristics of journal bearing,* Proceedings of the Institution of Mechanical Engineers, Part J: Journal of Engineering Tribology, vol. 229, iss. 10, pp. 1176–1186, 2015, doi: 10.1177%2F1350650115574734

[16] B.S. Shenoy, K.G. Binu, R. Pai, D.S. Rao, R.S. Pai, *Effect of nanoparticles additives on the performance of an externally adjustable fluid film bearing*, Tribology International, vol. 45, iss. 1, pp. 38-42, 2012, doi: 10.1016/j.triboint.2011.10.004

[17] R. Nicoletti, *The Importance of the Heat Capacity of Lubricants With Nanoparticles in the Static Behavior of Journal Bearings*, Journal of Tribology, vol. 136, iss. 4, p. 5, 2014, doi: 10.1115/1.4027861

[18] H. Montazeri, *Numerical analysis of hydrodynamic journal bearings lubricated with ferrofluid,* Proceedings of the Institution of Mechanical Engineers, Part J: Journal of Engineering Tribology, vol. 222, iss. 1, pp. 51–60, 2007, doi: 10.1243%2F13506501JET314

[19] P.B. Kushare, S.C. Sharma, *A study of two lobe non recessed worn journal bearing operating with non-Newtonian lubricant*, Proceedings of the Institution of Mechanical Engineers, Part J: Journal of Engineering Tribology, vol. 227, iss. 12, pp. 1418–1437, 2013, doi: 10.1177%2F1350650113496083

[20] S.C. Sharma, P.B. Kushare, *Two lobe non-recessed roughened hybrid journal bearing – A comparative study*, Tribology International, vol. 83, pp. 51–68, 2015, doi: 10.1016/j.triboint.2014.10.024

[21] X. Wang, *Thermohydrodynamic analysis of journal bearings lubricated with couple stress fluids,* Tribology International, vol. 34, iss. 5, pp. 335–343, 2001, doi: 10.1016/S0301-679X(01)00022-6

[22] Y. Aiman, S. Syahrullail, *Development of palm oil blended with semi synthetic oil as a lubricant using four-ball tester*, Jurnal Tribologi, vol. 13, pp. 1-20, 2017.

[23] S.R. Suryawanshi, J.T. Pattiwar, *Tribological performance of commercial Mobil grade lubricants operating with Titanium dioxide nanoparticle additives*, Industrial Lubrication and Tribology, vol. 71, iss. 2, pp. 188-198, 2018, doi: 10.1108/ILT-04-2018-0147

[24] R. Tiwari, *Rotor Systems: Analysis and Identification*, CRC Press, pp. 107-120, 2007.

[25] A. Harnoy, *Bearing Design in Machinery*, Marcel Dekker Inc. New York, pp. 144-172, 2002.

[26] D.D. Fuller, *Theory and Practice of Lubrication for Engineers*, New York: Wiley, pp. 271-282, 1984.

Nomenclature

c	Radial clearance, mm
C	Diametrical clearance, mm
e	Eccentricity, mm
g	Acceleration due to gravity, m/s^2
h	Oil variable film thickness, mm
ε	Eccentricity ratio
h_m	Minimum oil film thickness, mm
h_o	Film thickness at the point of peak pressure, mm
D	Diameter of journal, mm
R	Radius of journal, mm
L	Length of bearing, mm
N	Rotational speed of journal, r.p.m.
n	Rotational speed of journal, r.p.s.
ω	Angular velocity, rad/sec.
P	Bearing pressure, kPa
p	Pressure on fluid film, kPa
W	External load acting on shaft, N
μ	Dynamic viscosity, MPa-s
θ	Angular coordinates, degree
U	Journal surface velocity, m/s
ϕ	Attitude angle, degree
f	Bearing frictional coefficient
ΔT	Temperature rise in a film, °C
Q	Flow rate, m^3/s
Q_s	Side flow rate, m^3/s
ε_1	Eccentricity ratio at upper lobe for an elliptical bearing
ε_2	Eccentricity ratio at lower lobe for an elliptical bearing

ϕ_1	Attitude angle of upper lobe for an elliptical bearing, degree
ϕ_2	Attitude angle of lower lobe for an elliptical bearing, degree
C_h	Horizontal clearance for an elliptical journal bearing, mm
C_m	Minimum clearance when the center of shaft coincides with the center of elliptic bearing, mm
E_m	Elliptic ratio
R_U	Radius of upper lobe for an elliptical bearing, mm
R_L	Radius of lower lobe for an elliptical bearing, mm
m	Preload ratio
F_X	Dynamic force in X direction, N
F_Y	Dynamic force in Y direction, N
Δx	Displacement gradient in X direction, mm
Δy	Displacement gradient in Y direction, mm
$\Delta \dot{x}$	Velocity gradient in X direction, mm/s
$\Delta \dot{y}$	Velocity gradient in Y direction, mm/s
k_{XX}	Stiffness coefficient in X-X direction, N/m
k_{XY}	Stiffness coefficient in X-Y direction, N/m
k_{YX}	Stiffness coefficient in Y-X direction, N/m
k_{YY}	Stiffness coefficient in Y-Y direction, N/m
c_{XX}	Damping coefficient in X-X direction, Ns/m
c_{XY}	Damping coefficient in X-Y direction, Ns/m
c_{YX}	Damping coefficient in Y-X direction, Ns/m
c_{YY}	Damping coefficient in Y-Y direction, Ns/m

Abbreviations

NP	Nanoparticle
COF	Coefficient of Friction
WSD	Wear Scar Diameter
AC	Alternating Current
MCB	Miniature Circuit Breaker
LM	Linear Bushing
ASTM	American Society for Testing and Materials
IS	International Standards
GDQ	Generalized Differential Quadrature
CFD	Computational Fluid Dynamics
VFD	Variable Frequency Drive
FEM	Finite Element Method
FSI	Fluid Structure Interaction
ADI	Alternating Direction Implicit
FFT	Fast Fourier Transform
PTFE	Polytetrafluoroethylene
CMRO	Chemically Modified Rapeseed Oil
NC	Numerically Controlled
COC	Cleveland Open Cup
BSP	British Standard Pipe
psi	Pound per square inch
hp	Horse power
max.	Maximum
Theo.	Theoretical
Expt.	Experimental